

# PROCEEDINGS OF SPIE

[SPIDigitalLibrary.org/conference-proceedings-of-spie](https://spiedigitallibrary.org/conference-proceedings-of-spie)

## Front Matter: Volume 10453

**SPIE.**

PROCEEDINGS OF SPIE

# ***Third International Conference on Applications of Optics and Photonics***

**Manuel F. M. Costa**  
*Editor*

**8–12 May 2017**  
**Faro, Portugal**

*Organized by*  
SPOF—Sociedade Portuguesa para a Investigação e Desenvolvimento em Óptica e Fotónica  
"Portuguese Society for Optics and Photonics" (Portugal)

*Sponsored by*  
ICO—International Commission for Optics • EOS—European Optical Society •  
RIAO/SOPHIA—Red(e) Iberoamericana de Óptica • SEDOPTICA—Sociedad Española de  
Óptica (Spain) • AMO—Academia Mexicana de Óptica (Mexico) • RCO—Red Colombiana  
de Óptica (Colombia) • OPSS—Optics and Photonics Society of Singapore (Singapore)  
CVO—Comité Venezolano de Optica (Venezuela) • Innova Scientific, S.L. (Spain) • M.T.  
Brandão, Lda. (Portugal) • SOFE – Sociedad de Optica Y Fotonica del Ecuador (Ecuador)

*Cooperating Organization and Publisher*  
SPIE

**Volume 10453**

Proceedings of SPIE 0277-786X, V. 10453

SPIE is an international society advancing an interdisciplinary approach to the science and application of light.

Third International Conference on Applications of Optics and Photonics, edited by Manuel F. M. Costa,  
Proc. of SPIE Vol. 10453, 1045301 · © 2017 SPIE · CCC code: 0277-786X/17/\$18 · doi: 10.1117/12.2287443

Proc. of SPIE Vol. 10453 1045301-1

The papers in this volume were part of the technical conference cited on the cover and title page. Papers were selected and subject to review by the editors and conference program committee. Some conference presentations may not be available for publication. Additional papers and presentation recordings may be available online in the SPIE Digital Library at [SPIDigitalLibrary.org](http://SPIDigitalLibrary.org).

The papers reflect the work and thoughts of the authors and are published herein as submitted. The publisher is not responsible for the validity of the information or for any outcomes resulting from reliance thereon.

Please use the following format to cite material from these proceedings:

Author(s), "Title of Paper," in *Third International Conference on Applications of Optics and Photonics*, edited by Manuel F. M. Costa, Proceedings of SPIE Vol. 10453 (SPIE, Bellingham, WA, 2017) Seven-digit Article CID Number.

ISSN: 0277-786X  
ISSN: 1996-756X (electronic)

ISBN: 9781510613836  
ISBN: 9781510613843 (electronic)

Published by  
**SPIE**  
P.O. Box 10, Bellingham, Washington 98227-0010 USA  
Telephone +1 360 676 3290 (Pacific Time) · Fax +1 360 647 1445  
[SPIE.org](http://SPIE.org)

Copyright © 2017, Society of Photo-Optical Instrumentation Engineers.

Copying of material in this book for internal or personal use, or for the internal or personal use of specific clients, beyond the fair use provisions granted by the U.S. Copyright Law is authorized by SPIE subject to payment of copying fees. The Transactional Reporting Service base fee for this volume is \$18.00 per article (or portion thereof), which should be paid directly to the Copyright Clearance Center (CCC), 222 Rosewood Drive, Danvers, MA 01923. Payment may also be made electronically through CCC Online at [copyright.com](http://copyright.com). Other copying for republication, resale, advertising or promotion, or any form of systematic or multiple reproduction of any material in this book is prohibited except with permission in writing from the publisher. The CCC fee code is 0277-786X/17/\$18.00.

Printed in the United States of America.

Publication of record for individual papers is online in the SPIE Digital Library.

**SPIE. DIGITAL LIBRARY**  
[SPIDigitalLibrary.org](http://SPIDigitalLibrary.org)

**Paper Numbering:** *Proceedings of SPIE* follow an e-First publication model. A unique citation identifier (CID) number is assigned to each article at the time of publication. Utilization of CIDs allows articles to be fully citable as soon as they are published online, and connects the same identifier to all online and print versions of the publication. SPIE uses a seven-digit CID article numbering system structured as follows:

- The first five digits correspond to the SPIE volume number.
- The last two digits indicate publication order within the volume using a Base 36 numbering system employing both numerals and letters. These two-number sets start with 00, 01, 02, 03, 04, 05, 06, 07, 08, 09, 0A, 0B ... 0Z, followed by 10-1Z, 20-2Z, etc. The CID Number appears on each page of the manuscript.

# Contents

xi	<i>Authors</i>
xv	<i>Conference Committees</i>
xx	<i>Introduction</i>

---

## THIRD INTERNATIONAL CONFERENCE ON APPLICATIONS OF OPTICS AND PHOTONICS

---

10453 02	<b>Interchannel collisions of strong dispersion-managed solitons with different energies in the presence of higher-order effects</b> [10453-2]
10453 03	<b>Optical microtopographic inspection of asphalt pavement surfaces</b> [10453-3]
10453 04	<b>Spectrophotometric characterization of hemozoin as a malaria biomarker</b> [10453-5]
10453 05	<b>Low cost ellipsometer using a standard commercial polarimeter</b> [10453-6]
10453 06	<b>Generation of five phase-locked harmonics in the continuous wave regime and its potential application to arbitrary optical waveform synthesis</b> [10453-7]
10453 07	<b>Resonant tunneling diode photodetectors for optical communications</b> [10453-9]
10453 08	<b>Modelling of optoelectronic circuits based on resonant tunneling diodes</b> [10453-10]
10453 09	<b>Optical bias selector based on a multilayer <math>\alpha</math>-SiC:H optical filter</b> [10453-11]
10453 0A	<b>Visible light communication and indoor positioning using <math>\alpha</math>-SiCH device as receiver</b> [10453-12]
10453 0B	<b>Low-cost fused taper polymer optical fiber (LFT-POF) splitters for environmental and home-networking solution</b> [10453-13]
10453 0C	<b>Goos-Hänchen shift of Cosine-Gaussian Schell-model beams with rectangular symmetry</b> [10453-19]
10453 0D	<b>Simulation of localized surface plasmon in metallic nanoparticles embedded in amorphous silicon</b> [10453-21]
10453 0E	<b>Mode-locked semiconductor laser for long and absolute distance measurement based on laser pulse repetition frequency sweeping: a comparative study between three types of lasers</b> [10453-22]
10453 0F	<b>Erbium and ytterbium co-doped transparent oxyfluoride glass-ceramics optical fibers</b> [10453-24]

- 10453 0G **Fabrication and characterization of a cell electrostimulator device combining physical vapor deposition and laser ablation (Best Student Paper)** [10453-25]
- 10453 0H **Indoors positioning through VLC technology using an  $\alpha$ -SiC:H photodetector** [10453-26]
- 10453 0I **Critical discussion on the UV absorption properties of Earth's atmosphere** [10453-28]
- 10453 0J **Energy transfer between silver clusters and europium  $\text{Eu}^{3+}$  ions in photo-thermo-refractive glasses** [10453-30]
- 10453 0K **Optical, colloidal and biological properties of up-converting nanoparticles embedded in polyester nanocarriers** [10453-32]
- 10453 0L **Indirect gonioscopy system for imaging iridocorneal angle of eye** [10453-35]
- 10453 0M **On the behavior of linear polarizers on highly focused radially polarized beams** [10453-39]
- 10453 0N **Laser based manufacturing of channels and improvement of their lifetime with sol-gel coatings** [10453-40]
- 10453 0O **Validation of a semi-automatic protocol for the assessment of the tear meniscus central area based on open-source software** [10453-41]
- 10453 0P **Ferrofluids with high dynamic ranges of optical transmission** [10453-43]
- 10453 0Q **Photonic integrated circuits for NG-EPON** [10453-48]
- 10453 0R **Special microstructured fibers with irregular and regular claddings for supercontinuum generation** [10453-49]
- 10453 0S **Modeling multicore integrated waveguides in highly doped glass** [10453-50]
- 10453 0T **Clinical performance of an objective methodology to categorize tear film lipid layer patterns** [10453-51]
- 10453 0U **Color-quality control using color-difference formulas: progress and problems (Invited Paper)** [10453-56]
- 10453 0V **Electromagnetic properties of a monolayer of polarisable particles deposited on graphene (Runner Up Best Student Paper)** [10453-59]
- 10453 0W **Quantification of the absorption of light in coals using fiber optic sensors** [10453-60]
- 10453 0X **Modeling of dynamics of nanosecond laser ablation in phase explosion regime** [10453-61]
- 10453 0Y **Continual and molecular dynamics approaches in determining thermal properties of silicon** [10453-62]
- 10453 0Z **Electromagnetic simulation of amorphous silicon waveguides** [10453-63]
- 10453 10 **Wavemeter improvements for laser diode calibration (Invited Paper)** [10453-65]

- 10453 11 **Space-time refraction of light in time dependent media: the analogue within the analogue (Invited Paper)** [10453-66]
- 10453 12 **Surface enhanced Raman spectroscopy analysis of HeLa cells using a multilayer substrate** [10453-67]
- 10453 13 **Scattering, absorption and transmittance of experimental graphene dental nanocomposites** [10453-68]
- 10453 14 **The analogue quantum mechanical of plasmonic atoms** [10453-74]
- 10453 15 **Solving the multi-level Maxwell-Bloch equations using GPGPU computing for the simulation of nonlinear optics in atomic gases** [10453-77]
- 10453 16 **Doppler broadening effects in plasmonic quantum dots** [10453-78]
- 10453 17 **Development of a quantum particle in cell algorithm in GPU for solving Maxwell-Bloch equations** [10453-79]
- 10453 18 **Fast physical ray-tracing method for gravitational lensing using heterogeneous supercomputing in GPGPU** [10453-80]
- 10453 19 **Ultrasensitive detection of phenolic antioxidants by surface enhanced Raman spectroscopy** [10453-81]
- 10453 1A **Tunable light fluids using quantum atomic optical systems** [10453-84]
- 10453 1B **Pinching optical potentials for spatial nonlinearity management in Bose-Einstein condensates** [10453-85]
- 10453 1C **Dissipative solitons in 4-level atomic optical systems** [10453-86]
- 10453 1D **Wavefront coding for visual optics** [10453-87]
- 10453 1E **SPaCe-GEM: solver of the Einstein equations using GPUs under the gravitoelectromagnetic approximation** [10453-90]
- 10453 1F **The extended Kubelka-Munk theory and its application to colloidal systems** [10453-92]
- 10453 1G **Modelling metal-dielectric core-shell nanoparticles with effective medium theories** [10453-93]
- 10453 1H **Image encryption scheme based on computer generated holography and time-averaged moiré** [10453-94]
- 10453 1I **Effect of cooling water on ablation in Er:YAG laserosteotome of hard bone** [10453-95]
- 10453 1J **Mueller matrix imaging and analysis of cancerous cells** [10453-97]
- 10453 1K **Evaluation of FEL lamp seasoning behavior for use as a spectral irradiance standard** [10453-98]

- 10453 1L **Physical ray-tracing method for anisotropic optical media in GPGPU** [10453-99]
- 10453 1M **First approach on the Haar Transform applied with a 2 x 2 multimode interferometer** [10453-100]
- 10453 1N **Partially polarized pseudo-Schell model sources** [10453-102]
- 10453 1O **Studying tunability of some NIR semiconductor lasers by external cavity setup** [10453-103]
- 10453 1P **Interocular suppression** [10453-108]
- 10453 1Q **Optical quasi-distributed simultaneous vibration and temperature sensing in stator bars of a 370-MVA electric generator** [10453-110]
- 10453 1R **Refractive index sensitivity in etched FBG in the visible range** [10453-114]
- 10453 1S **Effect of laser pulse duration on ablation efficiency of hard bone in microseconds regime** [10453-115]
- 10453 1T **Towards the automatization of the Foucault knife-edge quantitative test** [10453-118]
- 10453 1U **Simulation of partially coherent light propagation using parallel computing devices** [10453-120]
- 10453 1V **Study of photo activation reaction of experimental graphene dental nanocomposites through dynamic laser speckle** [10453-123]
- 10453 1W **Variable structure and sliding modes nonlinear control system applied to a fiber optic interferometer** [10453-124]
- 10453 1X **A model for prediction of color change after tooth bleaching based on CIELAB color space** [10453-125]
- 10453 1Y **Finite element model for the simulation of laser activated micro- and nano-scale drug delivery systems** [10453-126]
- 10453 1Z **Short-length long period fiber grating for torsion sensing applications** [10453-127]
- 10453 20 **Spatio-temporal processing of ultra-short pulses with micro optics (Invited Paper)** [10453-129]
- 10453 21 **Fabry-Perot interferometer based on array of microspheres for temperature sensing (Invited Paper)** [10453-136]
- 10453 22 **Using DSLR cameras in digital holography** [10453-137]
- 10453 23 **Full Poincaré beams obtained by means of uniaxial crystals** [10453-140]
- 10453 24 **Simultaneous measurement of temperature and refractive index based on microfiber knot resonator integrated in an abrupt taper Mach-Zehnder interferometer** [10453-141]
- 10453 25 **Thermal sensitivity increase of RFBG in the visible range** [10453-142]

- 10453 26 **Strain sensor based on hollow microsphere Fabry-Perot cavity** [10453-144]
- 10453 27 **Dental resins properties studied by Bragg gratings (Invited Paper)** [10453-146]
- 10453 28 **Infrared light sensor applied to early detection of tooth decay** [10453-148]
- 10453 29 **Influence of a perturbation in the Gyrator domain for a joint transform correlator-based encryption system** [10453-153]
- 10453 2A **The USC-OSA-EPS section activities in optics** [10453-154]
- 10453 2B **Direct formation of nanostructures by focused electron beam on a surface of thin metallic films** [10453-156]
- 10453 2C **Rapid Eye Movements (REMs) and visual dream recall in both congenitally blind and sighted subjects (Invited Paper)** [10453-158]
- 10453 2D **Assessing the wavefront aberrations of the emmetropic eye after a reading task** [10453-161]
- 10453 2E **Strong coupling effects in hybrid plexitonic systems (Invited Paper)** [10453-163]
- 10453 2G **An exploratory study of temporal integration in the peripheral retina of myopes** [10453-171]
- 10453 2H **Organic semiconductor rubrene thin films deposited by pulsed laser evaporation of solidified solutions** [10453-176]
- 10453 2I **MIMO processing based on higher-order Poincaré spheres** [10453-177]
- 10453 2J **Optical properties of an anterior lamellar human cornea model based on fibrin-agarose** [10453-179]
- 10453 2K **2.05- $\mu\text{m}$  Holmium-doped all-fiber continuous-wave laser at in-core diode-pumping at 1.125  $\mu\text{m}$**  [10453-180]
- 10453 2L **Evaluating polarization diversity for speckle reduction in retinal image quality estimates** [10453-183]
- 10453 2M **Researching in biomaterials optics (Invited Paper)** [10453-186]
- 10453 2N **Modeling and possible implementation of self-learning equivalence-convolutional neural structures for auto-encoding-decoding and clusterization of images** [10453-187]
- 10453 2O **Photo-induced ultrasound microscopy for photo-acoustic imaging of non-absorbing specimens** [10453-189]
- 10453 2P **Electrical addressing and temporal tweezing of localized pulses in passively mode-locked semiconductor lasers (Invited Paper)** [10453-190]
- 10453 2Q **Resonant tunneling diode oscillators for optical communications** [10453-193]

- 10453 2R **White light spectral interferometer for measuring dispersion in the visible-near infrared** [10453-199]
- 10453 2S **Impact of different environmental conditions on lithium-ion batteries performance through the thermal monitoring with fiber sensors** [10453-200]
- 10453 2T **Phase contrast imaging of red blood cells using digital holographic interferometric microscope** [10453-202]
- 10453 2U **Fourier transform phase difference method optimization for supersonic gas flow characterization** [10453-203]
- 10453 2V **Fabry-Perot cavity based on air bubble for high sensitivity lateral load and strain measurements** [10453-204]
- 10453 2W **Polymer and tapered silica fiber connection for polymer fiber sensor application** [10453-205]
- 10453 2X **Onion cell imaging by using Talbot/self-imaging effect** [10453-208]
- 10453 2Y **Resonant tunnelling diode based high speed optoelectronic transmitters** [10453-209]
- 10453 2Z **THz metrology for active electronic devices: state of the art and challenges** [10453-211]
- 10453 30 **Effect of periodicity in the optimization of fine tuned dipolar plasmonic structures for SERS** [10453-213]
- 10453 31 **An advanced arrangement of the optical spectrograph based on acousto-optical and cross-disperser techniques for astronomical applications** [10453-217]
- 10453 32 **Analytical transient analysis of Peltier device for laser thermal tuning** [10453-221]
- 10453 33 **Wavelength tuning of polymer optical fibre Bragg grating at longer wavelengths permanently** [10453-224]
- 10453 34 **Novel multiband polarization beam splitter based on a dual-core transversally chirped microstructured optical fiber** [10453-229]
- 10453 35 **Electro-thermal effects in large area white-organic light emitting diodes** [10453-230]
- 10453 36 **Nonlinear joint transform correlator architectures for images encryption, decryption and authentication systems** [10453-236]
- 10453 37 **Design of low loss photonic crystal fiber based on porous-core with elliptical holes in THz regime** [10453-237]
- 10453 38 **Detection of low frequency, out-of-plane vibrations by the Talbot effect and adaptive photodetectors** [10453-238]

- 10453 39 **Multi-arm spectrometer for parallel frequency analysis of radio-wave signals oriented to astronomical observations** [10453-240]
- 10453 3A **Usage of CISS and Conlon surveys in eye accommodation studies** [10453-241]

## Authors

Numbers in the index correspond to the last two digits of the seven-digit citation identifier (CID) article numbering system used in Proceedings of SPIE. The first five digits reflect the volume number. Base 36 numbering is employed for the last two digits and indicates the order of articles within the volume. Numbers start with 00, 01, 02, 03, 04, 05, 06, 07, 08, 09, 0A, 0B...0Z, followed by 10-1Z, 20-2Z, etc.

Abbasi, Hamed, 1I, 1O, 1S  
Ab-Rahman, Mohammad Syuhaimi, 0B  
Abreu, Manuel, 05, 0E  
Acosta, E., 1D  
Afseth, N., 19  
Agarwal, Shilpi, 2X  
Aguilar-Hernández, I. A., 12, 19  
Aizpurua, Javier, 2E  
Alaminos, Miguel, 2J  
Alcaraz de la Osa, R., 1F, 1G  
Aldana, Mikel, 2L  
Alegria, E., 0D  
Alnamat, Bilal S., 2R  
Alharbi, Khalid H., 07  
Al-Khalidi, Abdullah, 07, 2Q, 2Y  
Almaguer, C., 1D  
Almeida, A. L., 1C  
Almeida, Álvaro J., 32  
Álvarez, Ezequiel, 0N  
Alves, R. A., 14, 15, 16, 17, 18, 1A, 1B, 1C, 1E, 1L  
Amorín, Adán, 2A  
Antona, Beatriz, 2C  
Aragón, Ángel L., 0G, 2A  
Arellanes, Adan Omar, 31, 39  
Arines, J., 1D  
Arosa, Yago, 2R  
Augustyn, Elżbieta, 0F  
Aung, Tin, 0L  
Aymerich, María, 0N, 2A  
Bani, Mohammad Amin, 1O  
Bao-Varela, Carmen, 0G, 2A  
Baptista, António M. G., 2G  
Barmenkov, Yuri O., 2K  
Barrio, Ana, 2C  
Baskaran, Mani, 0L  
Bastos, Ricardo, 32  
Bazylińska, Urszula, 0K  
Beltrán, Lina, 1I, 1S  
Benedicto, David, 0S  
Benjumea, Eberto, 28  
Berbel, M. A., 0C  
Bértolo, Helder, 2C  
Bierlich, Jörg, 2I  
Blanco, Manuel, 2A  
Blanco García, Jesús, 10, 2U  
Botero-Cadavid, Juan F., 37  
Cabral, Alexandre, 0E  
Camelin, P., 2P  
Cambronero-López, Ferran, 2A  
Cantu, Horacio, 2Q  
Cardona, Juan de la Cruz, 2J, 2M  
Cardozo da Silva, Jean Carlos, 1Q  
Carnicer, Artur, 0M  
Castañeda-Quintero, Raul, 2L  
Castro Alves, D., 0E  
Catarino, Susana O., 04  
Cattin, Philippe C., 1I, 1S  
Cerezo, V., 03  
Chavez Dagostino, Miguel, 39  
Chavushyan, Vahram, 3I  
Chiamenti, Ismael, 1R, 25  
Coelho, João M. P., 1Y, 1Z  
Contreras-Torres, F. F., 19  
Correa, Nelson, 2L  
Costa, J. C., 0H, 11, 14, 15, 16, 17, 18, 1A, 1B, 1C, 1E, 1L  
Costa, Manuel F. M., 03  
Cui, G., 0U  
Cunillera, A., 0C  
Czerska, Elwira, 0F  
de la Fuente, Raul, 2R  
de la Rosa, I., 1T  
De La Rue, Richard M., 30  
Demin, M. M., 0X  
Delgado, Tamara, 2A  
de Moura, Camila Carvalho, 25  
de Oliveira, Valmir, 25  
de Sande, Juan Carlos G., 1N, 23  
Díaz, Leonardo, 0W, 28  
Díaz-Otero, F. J., 02  
Diz-Bugarin, J., 10  
Döhring, Thorsten, 0I  
Dreyer, Uilian José, 1Q  
Dudea, Diana, 13  
Encarnação, Tito J., 2G  
Espitia, José, 28  
Esteban, Ruben, 2E  
Fantoni, Alessandro, 0A, 0D, 0Z  
Feldmann, Jochen, 2E  
Fernandes, Gil M., 2I  
Fernandes, João, 1M  
Fernandes, M., 0D  
Fernández, A., 1F, 1J  
Fernández-Luna, J. L., 1J  
Fernández-Maloigne, C., 0U  
Ferreira, Antonio F. G., Jr., 1K  
Ferreira, Marta S., 21, 2S, 2V  
Ferreira, Miguel F. S., 2W

Ferreira, T. D., 1A  
 Figueiredo, José M. L., 07, 08, 2Q, 2Y  
 Flores-Arias, M. Teresa, 0N, 2A  
 Foot, James A., 07, 08  
 Franco, Sandra, 2D  
 Frazão, Orlando, 21, 24, 26, 2W  
 Freitas, E. F., 03  
 Friederich, N., 1S  
 Fu, Chan Yiu, 0L  
 Gallego, Daniel, 33  
 García, P. A., 0U  
 García-Resua, Carlos, 0O, 0T  
 García-Sucerquia, Jorge, 22  
 Gargello, Ana, 2A  
 Garzón, Ingrid, 2J  
 Gavara, T., 06  
 Gaviña, Jefry, 2L  
 Gazda, M., 2H  
 Gebert de Oliveira Franco, Ana Paula, 27  
 Gerbreeders, Vjaceslavs, 2B  
 Ghafoor, Moeen, 0J  
 Ghinea, Razvan, 13, 2J, 2M  
 Giraldez, Maria J., 0O, 0T  
 Giudici, M., 2P  
 Gomes, André D., 24, 2W  
 Gomes, J., 35  
 Gomes, M., 11, 14, 15, 16, 17, 18, 1A, 1B, 1C, 1E,  
 1L  
 Gómez-Varela, Ana I., 0N, 2A  
 Gomez, Freiman, 34  
 Gómez-Cardona, N., 34  
 Gómez-Robledo, L., 0U  
 González, F., 1F, 1G  
 González-Andrades, Miguel, 2J  
 Gori, Franco, 1N  
 Govyadinov, Alexander A., 2E  
 Grzelczak, Marek, 2E  
 Guerreiro, A., 11, 14, 15, 16, 17, 18, 1A, 1B, 1C, 1E,  
 1L  
 Guillan-Lorenzo, O., 02  
 Gunab, Hadi, 0B  
 Gutiérrez, Y., 1F, 1G  
 Guzman, Raphael, 1I  
 Hänninen, Pekka E., 2O  
 Harun, Mohd Hazwan, 0B  
 Herrera, Luis J., 1X, 2M  
 Herrera-Ramírez, Jorge, 22, 2L  
 Hincapié-Zuluaga, Diego, 22, 2L  
 Holmes-Smith, A. Sheila, 30  
 Hong, F.-L., 06  
 Huang, M., 0U  
 Illarramendi, María Asunción, 0R  
 Ionescu, Ana M., 2J, 2M  
 Ivanov, R., 1T  
 Jahns, J., 20  
 Janusas, Giedrius, 1H  
 Jaschinski, Wolfgang, 3A  
 Javaloyes, J., 2P  
 Jendrzewski, R., 2H  
 Johnson, Nigel P., 30  
 Juvells, Ignasi, 0M  
 Kalinowski, Hypolito José, 1R, 25, 27  
 Kamicawachi, Ricardo C., 1R  
 Karam, Leandro Zen, 27  
 Katsuragawa, M., 06  
 Kelly, Anthony E., 2Q  
 Kępińska, Mirosława, 0F  
 Khan, Gufran S., 2T  
 Kir'yanov, Alexander V., 2K  
 Kitano, Cláudio, 1W  
 Kobelke, Jens, 2I  
 Koepke, Czesław, 0F  
 Koho, Sami V., 2O  
 Korneev, N., 38  
 Koroleva, O. N., 0Y  
 Kowal, Dominik, 2W  
 Krasilenko, Vladimir, G., 2N  
 Krumina, Gunta, 3A  
 Kuhne, Jean F., 1R  
 Kulbacka, Julita, 0K  
 Kumar, M., 35  
 Kumar, Varun, 2T, 2X  
 Lamela Rivera, Horacio, 33  
 Lazarev, Alexander, A., 2N  
 Li, C., 0U  
 Lima, Mário, 0Q, 1M  
 Lima, Rui, 04  
 Lisiecki, Radosław, 0F  
 Liz-Marzán, Luis M., 2E  
 López-Lago, Elena, 2R  
 López-Luke, T., 12, 19  
 Loren Inácio, Patrícia, 1R, 25  
 Lourenço, Paulo, 0Z  
 Louro, P., 09, 0A, 0D, 0H  
 Lucena, Cristina, 1V  
 Macedo, Antonio F., 2G  
 Magalhães, Tiago C., 1U  
 Majewska, N., 2H  
 Majumdar, S., 2H  
 Maluenda, David, 0M, 1N  
 Marasanov, Dmitriy, 0J  
 Marconi, M., 2P  
 Martelli, Cicero, 1Q  
 Martín, J. C., 0P  
 Martin, Roberta I., 1W  
 Martínez, G., 1T  
 Martínez-Herrero, Rosario, 0C, 0M, 1N  
 Mazhukin, A. V., 0X, 0Y  
 Mazhukin, V. I., 0X, 0Y  
 McMeekin, Scott G., 30  
 Melgosa, M., 0U  
 Melnikau, Dzmitry, 2E  
 Mendonça, J. T., 1I  
 Mergo, Pawel, 2W  
 Mestre, Tiago, 2C  
 Millán, María S., 29, 36  
 Minas, Graça, 04  
 Minkovich, Vladimir P., 0R  
 Moldovan, Marionara, 13  
 Monteiro, Catarina S., 26

Moraes, José Carlos T. B., 1K  
 Moreno, F., 1F, 1G, 1J  
 Morillas, S., 0U  
 Muga, Nelson J., 2I  
 Murukeshan, V. M., 0L  
 Nadas, Rafael B., 1R  
 Naftaly, Mira, 2Z  
 Naim, Nani Fadzlina, 0B  
 Nakagawa, K., 06  
 Nascimento, Micael, 2S  
 Nazeri, Majid, 1O  
 Nespereira, Marta, 1Z  
 Nieto, Daniel, 0G  
 Nikitovich, Diana V., 2N  
 Nikonorov, Nikolay, 0J  
 Novais, Susana, 2V  
 Nunes, Amélia Fernandes, 1P  
 Ohae, C., 06  
 Oliveira, Cristina M., 2D  
 Ormelas-Soto, N., 12, 19  
 Ortiz, D., 1F, 1G  
 Outumuro, L., 10  
 Palevicius, Arvydas, 1H  
 Palevicius, Paulius, 1H  
 Panke, Karola, 3A  
 Pazos, Antonio, 0G  
 Pecho, Oscar E., 2M  
 Pedrosa-Rodríguez, L., 02  
 Pena-Verdeal, Hugo, 0O, 0T  
 Pereira, L., 35  
 Pereira, Rui M. S., 0V  
 Peres, Nuno, 0V  
 Pérez, Eliseo, 0G  
 Pérez, María del Mar, 13, 1V, 1X, 2J, 2M  
 Pérez-Cabré, Elisabet, 29, 36  
 Perinchery, Sandeep M., 0L  
 Pichardo-Molina, J. L., 12  
 Pinho, Pedro, 0Z  
 Pinto, A., 35  
 Pinto, Armando N., 2I  
 Pinto, João L., 2S, 2V  
 Piquero, Gemma, 1N, 23  
 Pospori, Andreas, 33  
 Pozo, Antonio M., 1V  
 Pulgar, Rosa, 1X  
 Ragulskis, Minvydas, 1H  
 Rakovich, Yury P., 2E  
 Rauter, Georg, 1I, 1S  
 Rebordão, José Manuel, 0E, 1U, 1Y, 1Z  
 Rei, João F. M., 07, 08  
 Reyes-Vera, Erick, 34, 37  
 Ribeiro, A., 0D  
 Richard, N., 0U  
 Rivas, María José, 1X, 2M  
 Rodrigues, Carla, 0Q  
 Rodrigues, Francisco, 0Q, 1M  
 Rodrigues, Gil C., 07, 08, 2Y  
 Rodríguez Fernández, Carlos Damian, 2R  
 Rodríguez Lorenzo, Francisco, 2U  
 Rodríguez, G., 1T  
 Rodríguez-Montero, P., 38  
 Sagias, Georgios, 33  
 Saiz, J. M., 1F, 1G, 1J  
 Sakamoto, João M. S., 1W  
 Salas, Marianne, 13, 1V  
 Sánchez-Iglesias, Ana, 2E  
 Sánchez-García, Ángel, 2A  
 Santana, Janiley, 1X  
 Santarsiero, Massimo, 1N, 23  
 Santos, Jaime E., 0V  
 Santos, José L., 21  
 Sanz, J. M., 1G  
 Sanz-Felipe, Á., 0P  
 Savateeva, Diana, 2E  
 Sawczak, M., 2H  
 Schmidt, Mikolaj K., 2E  
 Sgibnev, Yevgeniy, 0J  
 Shahpari, Ali, 32  
 Shakher, Chandra, 2T, 2X  
 Shapranov, A. V., 0X, 0Y  
 Sharp, Graham G., 30  
 Shcherbakov, Alexandre S., 31, 39  
 Sheikhnejad, Yahya, 32  
 Silva, Ivo, 04  
 Silva, Nuno A., 11, 14, 15, 16, 17, 18, 1A, 1B, 1C, 1E, 1L  
 Silva, Susana O., 26  
 Simon, Thomas, 2E  
 Śliwiński, G., 2H  
 Snikeris, Janis, 2B  
 Sotsky, Alexander B., 0R  
 Souto, André, 0V  
 Statkiewicz-Barabach, Gabriela, 2W  
 Suhaimi, N. Sheeda, 06  
 Sulaiman, Malik, 0B  
 Supian, L. S., 0B  
 Svede, Aiga, 3A  
 Tcarenkova, Elena, 2O  
 Teixeira, António L., 0Q, 1M, 32  
 Teixeira, Marcelo C. M., 1W  
 Tepichín Rodríguez, Eduardo, 31, 38, 39  
 Texeira, D., 0D  
 Torres, Cesar, 0W, 28  
 Torres, H., 03  
 Tuna, Ana Rita, 1P  
 Urban, Alexander S., 2E  
 Úsuga-Restrepo, J., 34, 37  
 Vaca Pereira G., M., 0R  
 Vagner da Silva, Erlon, 1Q  
 Valencia, J. L., 10  
 Vallés, Juan A., 0S  
 Vasilevskiy, Mikhail, 0V  
 Vázquez Dorrio, Benito, 10, 2U  
 Velosa, F., 05  
 Vieira, M., 09, 0A, 0D, 0H  
 Vieira, M. A., 09, 0A, 0H  
 Vieira, P., 0A  
 Vilaridy, Juan M., 0W, 29, 36  
 Vilarinho, Daniel, 2G  
 Vilhena, Henrique, 1Y, 30

Villa, J., 1T  
Villatoro, Joel, 0R  
Vujicic, Zoran, 32  
Vygranenko, Y., 0D  
Wang, Jue, 07, 2Q, 2Y  
Wasige, Edward, 07, 2Q, 2Y  
Watson, Scott, 2Q  
Wawrzyńczyk, Dominika, 0K  
Webb, David J., 33  
Williamson, Sandra, 2A  
Wiśniewski, Krzysztof, 0F  
Wold, J. P., 19  
Yebra, Ana, 13, 1V, 1X, 2M  
Yebra-Pimentel, Eva, 0O, 0T  
Zam, Azhar, 11, 1S  
Żelechower, Michał, 0F  
Zhang, Weikang, 2Q  
Zubia, Joseba, 0R  
Zuñiga-Bedoya, J., 37

## Conference Committees

### *Conference Chair*

**Manuel F. M. Costa**, Universidade do Minho (Portugal)

### *International Scientific Committee*

**Amparo Pons Martí**, Universidad de València (Spain)  
**Ana Consortini**, Università degli Studi di Firenze (Italy)  
**Anand Krishna Asundi**, Optics and Photonics Society of Singapore (Singapore) and Nanyang Technological University (Singapore)  
**Andrea Cusano**, Università degli Studi di Sannio (Italy)  
**Andrew Moore**, Herriot-Watt University (United Kingdom)  
**Andrés Márquez Ruiz**, Universidad de Alicante (Spain)  
**Angel Augier Calderin**, InSTEC–Instituto Superior de Tecnologías y Ciencias Aplicadas (Cuba)  
**Angel I. Negueruela**, Universidad de Zaragoza (Spain)  
**Angela M. Guzman**, CREOL, The College of Optics and Photonics, University of Central Florida (United States)  
**Asticio Vargas**, Universidad de La Frontera (Chile)  
**Carlos Ferreira**, Universidad de València (Spain)  
**Carlos Saavedra Rubilar**, Universidad de Concepción (Chile)  
**Cesar Augusto Costa Vera**, Escuela Politécnica Nacional (Ecuador)  
**Clementina Timus**, National Institute for Laser, Plasma, and Radiation Physics (Romania)  
**Cristiano M. B. Cordeiro**, Universidade Estadual de Campinas (Brazil)  
**Daniel Malacara Hernández**, Centro de Investigaciones en Óptica (Mexico)  
**Efraín Solarte Rodriguez**, RCO–Red Colombiana de Óptica (Colombia)  
**Eric Rosas**, Centro de Investigaciones en Óptica, A.C. (Mexico)  
**Eugene Arthurs**, SPIE  
**Gonçalo Figueira**, Universidade Nova de Lisboa (Portugal)  
**Guillermo Baldwin**, Pontificia Universidad Católica del Perú (Peru)  
**Hai-Ning Cui**, Jilin University (China)  
**Hector Rabal**, CIOp–Centro de Investigaciones Ópticas (Argentina)  
**Humberto Michinel**, Universidad de Vigo (Spain)  
**Hypolito Kalinowski**, Universidade Tecnológica Federal do Paraná (Brazil)  
**James Wyant**, College of Optical Sciences, The University of Arizona (United States)  
**Jana B. Nieder**, International Iberian Nanotechnology Laboratory (Portugal)  
**Jesús Lancis**, Universidad Jaume I (Spain)  
**Joaquín Campos Acosta**, CSIC–Instituto de Óptica (Spain)  
**João Lemos Pinto**, i3N–Institute of Nanostructures, Nanomodelling and Nanofabrication (Portugal)

**João Manuel Tavares**, Universidade do Porto (Portugal)  
**John Canning**, University of Sydney (Australia)  
**José António Rodrigues**, Universidade do Algarve (Portugal)  
**Jose Benito Vazquez-Dorrio**, Universidad de Vigo (Spain)  
**José Figueiredo**, Universidade do Algarve (Portugal)  
**José Luis Paz**, CTOV (Venezuela)  
**José Manuel de Nunes Vicente Rebordão**, Universidade Nova de Lisboa (Portugal)  
**José Ramiro Fernandes**, Universidade de Trás-os-Montes e Alto Douro (Portugal)  
**José R. Salcedo**, ATLA Lasers (Norway)  
**José Silva Gomes**, Universidade do Porto (Portugal)  
**Juan G. Darias Gonzalez**, Centro de Aplicaciones Tecnológicas y Desarrollo Nuclear (Cuba)  
**Luciano Alberto Angel-Toro**, RCO–Red Colombiana de Óptica (Colombia)  
**Luis Miguel Bernardo**, Universidade do Porto (Portugal)  
**Luis Roso**, Centro de Láseres Pulsados Ultracortos Ultraintensos (Spain)  
**Luis Silvino Alves Marques**, Universidade do Minho (Portugal)  
**Katrina Svanberg**, University of Lund (Sweden)  
**Kiyofumi Matsuda**, National Institute of Advanced Industrial Science and Technology (Japan)  
**Kim Chew Ng**, Monash University (Australia)  
**Manuel Lopez-Amo**, Universidad Pública de Navarra (Spain)  
**Manuel Melgosa Latorre**, Universidad de Granada (Spain)  
**Marcelo Trivi**, Universidad Nacional de Mar del Plata (Argentina)  
**Maria Josefa Yzuel**, Universidad Autònoma de Barcelona (Spain)  
**Maria Luisa Calvo**, Instituto de Credito Oficial (Spain)  
**Maria Sagrario Millan**, Universidad Politècnica de Catalunya (Spain)  
**Mário Vaz**, INEGI (Portugal)  
**Maité Flores-Arias**, Universidad de Santiago de Compostela (Spain)  
**Marta Maria Duarte Ramos**, Universidade do Minho (Portugal)  
**Miguel Gonzalez Herraes**, Universidad de Alcalá (Spain)  
**Mikiya Muramatsu**, Universidade de São Paulo (Brazil)  
**Mikhail I. Vasilevski**, Universidade do Minho (Portugal)  
**Mourad Zghal**, STO–Société Tunisienne d'Optique (Tunisia)  
**Mustafa Erol**, Bozok University (Turkey)  
**Pablo Artal**, Universidad de Murcia (Spain)  
**Paulo Torrao Fiadeiro**, Universidade da Beira Interior (Portugal)  
**Paulo J. da Silva Tavares**, Universidade do Porto (Portugal)  
**Pedro Andrés Riao**, Universidad de València (Spain)  
**Radu Chisleag**, Technical University of Bucharest (Romania)  
**Ramón Rodríguez-Vera**, Centro de Investigaciones en Óptica, A.C. (Mexico)  
**Raul Rangel**, Centro de Investigación Científica y de Educación Superior de Ensenada B.C. (Mexico)  
**Rastogi Pramod**, École Polytechnique Fédérale de Lausanne (Switzerland)  
**Robert Lieberman**, Lumoptix, LLC (United States)

**Roger Ferlet**, Université de Paris (France)  
**Salvador Bará**, Universidad de Santiago de Compostela (Spain)  
**Tomas Catunda**, Universidade de São Paulo (Brazil)  
**Sabry Abdel-Mottaleb**, Ain-Shams University (Egypt)  
**Santiago Vallmitjana Rico**, SEDOPTICA–Sociedad Española de Óptica (Spain) and Universidad de Barcelona (Spain)  
**Sun Tong**, City University (United Kingdom)  
**Toyohiko Yatagai**, Utsunomiya University (Japan)  
**Waclaw Urbanczyk**, Wrocław University of Technology (Poland)  
**Zuqing Zhu**, University of Science and Technology of China (China)

*Program Review Committee*

**António Baptista**, Universidade do Minho (Portugal)  
**António Lobo**, Universidade Fernando Pessoa (Portugal)  
**Benito Vázquez-Dorrío**, Universidad de Vigo (Spain)  
**Gonçalo Figueira**, Universidade de Lisboa (Portugal)  
**João M. P. Coelho**, Universidade de Lisboa (Portugal)  
**José António Rodrigues**, Universidade do Algarve (Portugal)  
**Manuel F. M. Costa**, Universidade do Minho (Portugal)  
**Manuel Melgosa Latorre**, Universidad de Granada (Spain)  
**Mikhail I. Vasilevskiy**, Universidade do Minho (Portugal)  
**Orlando Frazão**, Universidade do Porto (Portugal)  
**Paulo Torrão Fiadeiro**, Universidade da Beira Interior (Portugal)  
**Paulo J. da Silva Tavares**, Universidade do Porto (Portugal)  
**Rogério Nunes Nogueira**, Universidade de Aveiro (Portugal)

*Program Committee*

**Alexandre Cabral**, Universidade de Lisboa (Portugal)  
**Alicia Fernández Oliveras**, Universidad de Granada (Spain)  
**Amit Garg**, Acharya Narendra Dev College (India)  
**Ana Maria Rocha**, Instituto de Telecomunicações (Portugal)  
**Anand Krishna Asundi**, Optics and Photonics Society of Singapore (Singapore) and Nanyang Technological University (Singapore)  
**Angel Augier Calderin**, José Antonio Echevarría Higher Polytechnic Institute (Cuba)  
**Angela M. Guzman**, CREOL, The College of Optics and Photonics, University of Central Florida (United States)  
**António Baptista**, Universidade do Minho (Portugal)  
**António Lobo**, Universidade Fernando Pessoa (Portugal)  
**Carla Carmelo Rosa**, Universidade do Porto (Portugal)  
**Carlos Saavedra Rubilar**, Universidad de Concepción (Chile)  
**Cesar Augusto Costa Vera**, Escuela Politécnica Nacional (Ecuador)  
**Clementina Timus**, National Institute for Laser, Plasma and Radiation Physics (Romania)  
**Efraín Solarte Rodríguez**, RCO–Red Colombiana de Óptica (Colombia)  
**Eric Rosas**, Centro de Investigaciones en Óptica, A.C. (Mexico)  
**Gonçalo Figueira**, Universidade de Lisboa (Portugal)

**Hai-Ning Cui**, Jilin University (China)  
**Humberto Michinel**, Universidad de Vigo (Spain)  
**Ireneu Dias**, INESC Porto (Portugal)  
**Jana B. Nieder**, International Iberian Nanotechnology Laboratory (Portugal)  
**Joaquim Carneiro**, Universidade do Porto (Portugal)  
**João M. P. Coelho**, Universidade de Lisboa (Portugal)  
**João Manuel Tavares**, Universidade do Porto (Portugal)  
**Jose Benito Vazquez-Dorrio**, Universidad de Vigo (Spain)  
**José Figueiredo**, Universidade do Algarve (Portugal)  
**José Luis Paz**, National Polytechnic School (Venezuela)  
**José Luís Santos**, Universidade do Porto (Portugal)  
**José Manuel Baptista**, INESC Porto (Portugal)  
**José R. Salcedo**, ATLA Lasers (Norway)  
**José Silva Gomes**, Universidade do Minho (Portugal)  
**Lúcia Bilro**, Instituto de Telecomunicações (Portugal)  
**Luis Miguel Bernardo**, Universidade do Porto (Portugal)  
**Kim Chew Ng**, Monash University (Australia)  
**Manuel F. M. Costa**, Universidade do Minho (Portugal)  
**Manuel Joaquim Marques**, Universidade do Porto (Portugal)  
**Mário Lima**, Universidade de Aveiro (Portugal)  
**Naoya Wada**, National Institute of Information and Communications Technology (Japan)  
**Nélia Alberto**, Instituto de Telecomunicações (Portugal)  
**Orlando Frazão**, Universidade do Porto (Portugal)  
**Robert Lieberman**, Lumoptix, LLC (United States)  
**Rogério Nunes Nogueira**, Universidade de Aveiro (Portugal)  
**Susana Silva**, INESC-TEC (Portugal)

#### *Technical Chairs*

**António Baptista**, Universidade do Minho (Portugal)  
**Gonçalo Figueira**, Universidade de Lisboa (Portugal)  
**José António Rodrigues**, Universidade do Algarve (Portugal)  
**José Figueiredo**, Universidade do Algarve (Portugal)  
**Orlando Frazão**, Universidade do Porto (Portugal)  
**Paulo Torrao Fiadeiro**, Universidade da Beira Interior (Portugal)  
**Rogério Nunes Nogueira**, Universidade de Aveiro (Portugal)

## Introduction

Celebrating Optics and Photonics and its outstanding positive impact in the world and in our everyday life (largely resulting from the current remarkable success and fast sustainable development in optics and photonics research, the Portuguese Society for Optics and Photonics (Portugal), SPOF - Sociedade Portuguesa para a Investigação e Desenvolvimento em Óptica e Fotónica (Portugal)) successfully organised its third triennial international conference on Applications of Optics and Photonics, 8 – 12 May, at the Universidade do Algarve in the lovely city of Faro, Portugal.

The conference was organized to foster the establishment of the widest range of cooperation projects and relationships with colleagues and institutions from all around the world, while increasing the external visibility of Portugal's optics and photonics research.

The success of the conference came from the enthusiastic commitment of the Portuguese optics and photonics community and of our friends from all over the world, and the endorsement and active support of the most important international scientific optics societies:

ICO, SPIE, EOS, RIAO; several national societies, committees, and boards: SEDOPTICA- Sociedad Española de Óptica (Spain), AMO (Mexico), STO (Tunisia), OPSS (Singapore), CVO (Venezuela), RCO (Colombia), SOFE (Ecuador), and SPF (Portugal);

other photonics and optics industries and companies, as well as the following projects and initiatives: Laserlab-Europe, iBROW, INNOVA, Laser World of Photonics, OPA, OQEJ-Springer, adLASER, MTBrandão, Lda.;

and the contribution from the authors and presenters of the 191 effectively presented talks in all domains of optics and photonics.

Of the over two hundred works presented, the conference included 32 invited lectures from world leading scientists and 7 plenary lectures, which gave an excellent overview of the state of the art in optics and photonics research across the world pointing out perspectives of future developments.

Well over one third of all 149 effective participants of the conference were students. This percentage increased to nearly 50% among the Portuguese participants, illustrating the vitality and growth potential of research in optics and photonics in Portugal, and all over the world in general. The support of the International Commission for Optics helped the participation of seventeen students. EOS and SPIE awarded prizes, respectively, to the best student poster presentations and best student research works presented at the conference.

At the closing ceremony of the conference the 2014 and 2015 SPOF's Best PhD Thesis in Portugal in Optic and Photonics were awarded to Hugo Martins ("Distributed and Remote Fiber Sensing Assisted by Raman Effect") and to Marta Ferreira ("Fiber Sensing Based on New Structures and Post-Processing Enhancement"), both former students of the Universidade do Porto (Portugal).

Reflecting the development of the scientific and technological research in optics and photonics in Portugal over last decades and the success of the previous editions of SPOF's conference; it was decided to change the periodicity of our AOP conferences to biannual. Therefore our next conference will be held 3 – 7 June, 2019, in Lisbon, Portugal.

We are looking forward to another exciting and most enjoyable conference!

**Manuel F. M. Costa**



# PROCEEDINGS OF SPIE

[SPIDigitalLibrary.org/conference-proceedings-of-spie](https://spiedigitallibrary.org/conference-proceedings-of-spie)

## Validation of a semi-automatic protocol for the assessment of the tear meniscus central area based on open-source software

Hugo Pena-Verdeal  
Carlos Garcia-Resua  
Eva Yebra-Pimentel  
Maria J. Giraldez

**SPIE.**

# Clinical performance of an objective methodology to categorize tear film lipid layer patterns

Carlos Garcia-Resua\*<sup>a</sup>, Hugo Pena-Verdeal<sup>a</sup>, Maria J. Giraldez<sup>a</sup>, Eva Yebra-Pimentel<sup>a</sup>.

<sup>a</sup>Departamento de Física Aplicada (Area de Optometría), Universidade de Santiago de Compostela, Santiago de Compostela, Spain

## ABSTRACT

**Purpose:** To validate the performance of a new objective application designated iDEAS (Dry Eye Assessment System) to categorize different zones of lipid layer patterns (LLPs) in one image. **Material and methods:** Using the Tearscope-plus and a digital camera attached to a slit-lamp, 50 images were captured and analyzed by 4 experienced optometrists. In each image the observers outlined tear film zones that they clearly identified as a specific LLP. Further, the categorization made by the 4 optometrists (called observer 1, 2, 3 and 4) was compared with the automatic system included in iDEAS (5th observer). **Results:** In general, observer 3 classified worse than all observers (observers 1, 2, 4 and automatic application, Wilcoxon test,  $p < 0.05$ ). The automatic system behaved similar to the remaining three observers (observer 1, 2 and 4) showing differences only for Open meshwork LLP when comparing with observer 4 (Wilcoxon test,  $p = 0.02$ ). For the remaining two observers (observer 1 and 2) there was not found statistical differences (Wilcoxon test,  $p > 0.05$ ). Furthermore, we obtained a set of photographs per LLP category for which all optometrists showed agreement by using the new tool. After examining them, we detected the more characteristic features for each LLP to enhance the description of the patterns implemented by Guillon. **Conclusions:** The automatic application included in the iDEAS framework is able to provide zones similar to the annotations made by experienced optometrists. Thus, the manual process done by experts can be automated with the benefits of being unaffected by subjective factors.

**Keywords:** Lipid layer pattern; Tearscope-plus; Tear film; interference phenomena; image categorization.

## 1. INTRODUCTION

The lipid layer of the tear film plays a major role in limiting evaporation during the inter-blink period and also affects tear film stability. Tear film quality and lipid layer thickness can be assessed by non-invasively imaging the superficial lipid layer by interferometry and these two variables are correlated.[1] Guillon proposed five main grades of lipid layer thickness interference patterns for observations made using the Tearscope-plus (figure 1): open meshwork (OM), closed meshwork (CM), wave or flow (W), amorphous (AM) and colour fringe (CO). This author also described abnormal lipid layer patterns (LLPs)[2].

Although this method has proven useful to evaluate the quality and structure of the tear film,[1] it is affected by the subjective interpretation of the observer. Thicker lipid layers ( $\geq 90$  nm) are readily observed since they produce color and wave patterns. However, thin lipid layers ( $\leq 60$  nm) are difficult to visualize, since color fringes and other distinct morphological features are not present and their interpretation is more subjective.[3] Training also affects the interpretation of the LLPs and there is a learning curve for Tearscope tear interference pattern grading.[4]

In an effort to find a more objective way to classify the LLPs provided by the Tearscope, a new software application has been recently developed. Using this new software, several authors have reported good agreement among experienced observers[5] when interpreting LLPs and the method is currently the focus of a funded research project by the present authors.

Therefore, the purpose of this study, based on the objectives of the DEWS[6], was to validate the performance of an objective software application (iDEAS) to categorize different zones of LLPs in one image. The validation was done by comparing the zones of LLP categorization between all observers (4 experienced observers and the automatic system) in order to find out whether the five observers categorized similarly

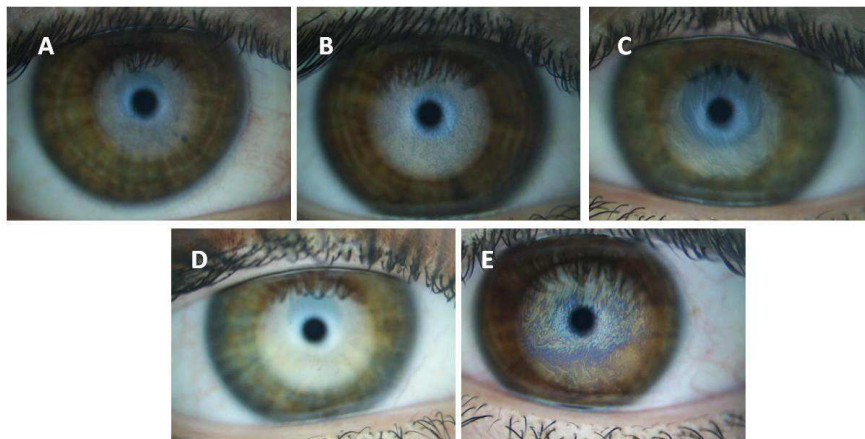


Figure 1. Lipid layer patterns as seen by Tearscope plus. A) Open meshwork, B) Closed meshwork, C) Wave, D) Amorphous and E) Color fringe.

## 2. MATERIAL AND METHODS

### 2.1 Subjects and procedure

Subjects were recruited among patients visiting the Optometry Clinic of the Optometry Faculty (Universidad de Santiago de Compostela, Spain) for an eye examination. Subjects were excluded if they had ocular infection or ocular allergy, were contact lens users, took a prescription eye medication, or were pregnant or breastfeeding. They were asked not to wear eye makeup prior to the clinical protocol. All subjects were given written information about the study before they signed a written statement of consent to participate. The study protocol adhered to the tenets of the Declaration of Helsinki and was revised and approved by the Ethics Committee of the University of Santiago de Compostela (Spain).

The tear film lipid layer was examined using a Tearscope-plus<sup>®</sup> (Keeler, Windsor, UK). This instrument, designed by Guillon, is the instrument most commonly used in clinical practice for the rapid assessment of lipid layer thickness and has been described in detail elsewhere.[1] Briefly, the Tearscope projects a cylindrical source of cool white fluorescent light onto the lipid layer. Thus, any observed phenomena are unique to the specific light source of the Tearscope.

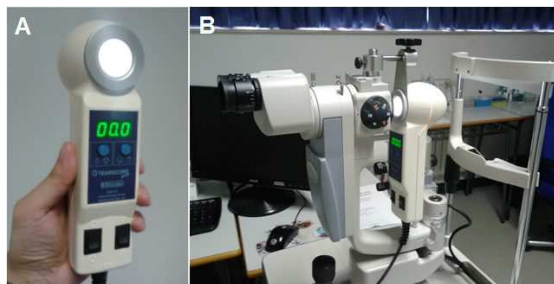


Figure 2. Tearscope plus. This device enables specular reflection over the entire cornea through a cylindrical source of white fluorescent light onto the lipid layer. a) Tearscope plus hand-held instrument. b) Tearscope plus attached to a slit lamp, which enables high magnification.

Tearscope was attached to a Topcon SL-D4 slit lamp with a R900 Goldmann tonometer support (figure 2). The slit-lamp magnification was set at x16 and illumination was that provided by the Tearscope (the slit lamp source is not switched on). Tearscope offers two sets of illumination; in all the measurements we chose the brightest one.

To capture LLPs videos a Topcon DV-3 digital camera was used and attached to the slit lamp. All videos were stored in a computer via Topcon IMAGENet i-base software at a spatial resolution of 1024 x 768 pixels in the RGB color space.

All images were then uploaded to the database included in the iDEAS software for image classification. Around 2000 images were uploaded in the iDEAS database at the time of the study. Then, a set of images that better fulfilled the quality requirements (free of blur, lipid layer well spread after a complete blink and well centered) were selected. This yielded 50 images that were used for our study.

## 2.2. iDEAS

iDEAS (Dry Eye Assessment System) is a web application designed to join several services in the field of optical image processing.[7] For the reader's interest, a wide description of the iDEAS framework is indicated elsewhere, where the technical features are indicated in detail.[8] Here it was described the functionalities that were used in this study.

Regarding the image tools, it has two main functionalities. On the one hand, by clicking the classify icon on an image, the application classifies the tear film image and assigns a specific LLP type to the whole image. This automatic classification tool has been proposed elsewhere,[9, 10] and was properly validated by optometrists by comparing LLP classifications of 105 images with those provided by 3 observers.[5]

On the other hand, by clicking the annotation icon on an image, the web application allows users to manually trace different regions associated each one with a specific LLP. The observer only has to click and drag a pointer on the image to delineate a region. This determines that an image of several discrete LLP zones can be subjectively categorized in one image. The importance of this functionality lies in the fact that the lipid layer of the tear film may show a multiple LLP (representing various lipid thicknesses), which indicates, as Guillon reported this is a sign of a meibomian gland abnormality[1] and suggests that the regularity of the LLP is a useful clinical sign.

In this sense, a new automatic tool is being developed in order to identify several LLP zones in a single patient image. First attempt to achieve this goal was presented earlier,[11] based on the techniques for color texture analysis used previously[10] and decision voting system. However, the main problem of this first approach is that it uses the unreal background category, which represents the areas of the images in which there is no LLP. Thus, the method proposed here consists of a weighted voting system which takes into account the class-membership probabilities provided by a soft classifier, and uses a minimum threshold to distinguish the background from the Guillon categories without using any unreal category. Preliminary results demonstrate the feasibility of this new tool, which will enhance the applications of the Tearscope and offer the clinician and researcher a not too sophisticate device to assess quality aspects of the tear film.

The research methodology proposed to create tear film maps based on the lipid interference patterns consists of five stages (Figure 3).

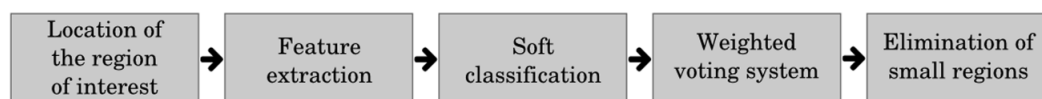


Figure 3. Scheme of the research methodology to create tear films maps.

The input data is a tear film image acquired with the Tearscope-plus, and the output data is a labeled image based on the interference patterns defined by Guillon. Firstly, the region of interest, in which the further analysis will take place, is located. Next, each local window inside it is analyzed in terms of color and texture features, and its class-membership probabilities are calculated by using a soft classifier. Following, the segmentation is performed using the weight voting system in such a way that every pixel of every window receives a vote associated to each class  $c$ :

$$v_c = w_1 \cdot p_c + w_2 \cdot p_c / d$$

where  $p_c$  is the probability of belonging to the class  $c$ ,  $d$  is the distance from the pixel to the center of the window, and  $w_1$  and  $w_2$  weight the probability and the distance, respectively. As windows are overlapped, each pixel belongs to several categories and so the votes received from each category are added up. Thus, the pixel is assigned to the most voted category only if its total number of votes is greater than a threshold. Finally, the tear film map obtained is post-processed in order to eliminate the small regions which usually correspond to false positives or noisy areas.

### 2.2.1. Characterization of the lipid layer patterns

Both image tools available in the iDEAS web system are based on the characterization of the lipid layer patterns by means on color and texture information. Broadly speaking, color and interference patterns are the two discriminant features of the Guillon categories for lipid layer assessment. On the one hand, some categories show distinctive color characteristics which motivate the color analysis step. On the other hand, the interference phenomena can be characterized as a texture pattern, since thicker lipid layers show defined patterns while thinner layers are more homogeneous.

For color analysis, the use of the Lab color space is considered according to previous research.[12] The CIE 1976 L\*a\*b color space[13] (Lab) is a chromatic color space which describes all the colors that the human eye can perceive. It was defined by the International Commission on Illumination, abbreviated as CIE from its French title Commission Internationale de l'Eclairage. Lab is a 3D model where its three coordinates represent: the luminance of the color L, its position between magenta and green a, and its position between yellow and blue b. Its use is recommended by CIE in images with natural illumination. In addition, this color space is perceptually uniform, a very important characteristic since experts' perception is trying to be imitated. The use of the Lab color space entails converting the three channels of the Tearscope image in RGB into the three components of Lab, which will be subsequently analyzed in terms of texture.

Regarding texture analysis, the co-occurrence features technique is applied due to its effectiveness to characterize the LLPs.[12] Co-occurrence features[14] allow to define a texture descriptor based on the computation of the conditional joint probabilities of all pair wise combinations of gray levels, given an interpixel distance and an orientation. The method generates a set of gray level co-occurrence matrices (GLCM), and extracts several statistical measures from their elements. The Chebyshev distance is here considered and, in general, the number of matrices for a distance  $d$  is  $4d$ . From each GLCM, a set of 14 statistical measures proposed by Haralick et al.[14] are computed, which represent features such as contrast or homogeneity. Finally, the mean and the range of these 14 statistics are calculated across matrices and a set of 28 features composes the texture descriptor for a particular distance.

### 2.3. Pattern classifications. Agreement among 4 experienced observer's methodology

Four observers experienced in LLP grading were asked to categorize the LLPs found in 50 images selected as described above (section 2.1). In each image, the observer marked the LLP zones of interest using the iDEAS tool (Figure 4a). The iDEAS program was then used to extract the zones for which there was agreement among all 4 observers (Figure 4b). These agreed areas were catalogued as "correct images" to be included in the database created to guide LLP categorization.

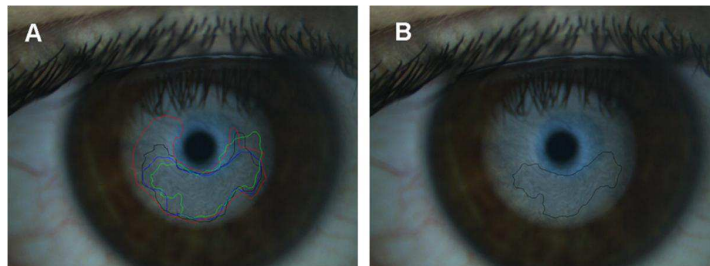


Figure 4. Image interpreted by 4 observers using the iDEAS. A) Overlapping zones marked by the observers; each color indicates the zone categorized by one observer. B) Zone for which there was agreement among the 4 observers.

### 2.4. Data and statistical analysis

In order to validate this new application, the system was compared with the annotations made by four experienced observers. This validation process consists in dealing with the system as it was another observer, and so a comparison between five hypothetical observers was performed. In this manner, the areas marked by a reference observer were compared with the areas annotated by the other four observers. That is, the number of pixels of the reference observer which match with other observers are added up and graphically represented. Therefore, if the reference observer is compared with the rest of observers, there are a number of pixels in which the reference observer agrees with 0, 1, 2, 3 or 4 observers. Thus, the agreement with 4 observers means a total agreement between the five hypothetical observers considered, whilst the agreement with 0 observers implies that those pixels were marked only by the reference observer.

This comparison between experts was performed in such a way that each observer is used as the reference observer once, and so a total of five comparisons are obtained.

As an example, figure 5 illustrates the annotations made by the 4 observers over 5 representative images, and their respective output images provided by the automatic system. As can be seen, there are areas of the images in which the observers agree with the LLP, whereas there are other areas in which there is no agreement. The same situation can be appreciated if the output images are compared with the observers' annotations.

The size of *Perfect categorization (PC)* (those pixels in agreement between reference observer and the all remaining 4 observers) was not considered, because all the five observers show the same value. Therefore, the analysis of the comparisons was performed considering the *Erroneous categorization (EC)*, that is, those pixels that reference observer observed agreed with 0 observers or were marked only by the reference observer, where the lower the size of the EC area, the better the performance of LLP categorization.

Kolmogorov-Smirnov test was done for each variable and it was found that they did not follow a normal distribution ( $p < 0.05$ ), so non parametric statistics were used. In order to perform multiple comparisons a Kruskal-Wallis test was used. Finally, to perform pair wise comparisons, Friedman test was used for independent variables whereas a Wilcoxon test was used for dependent variables.

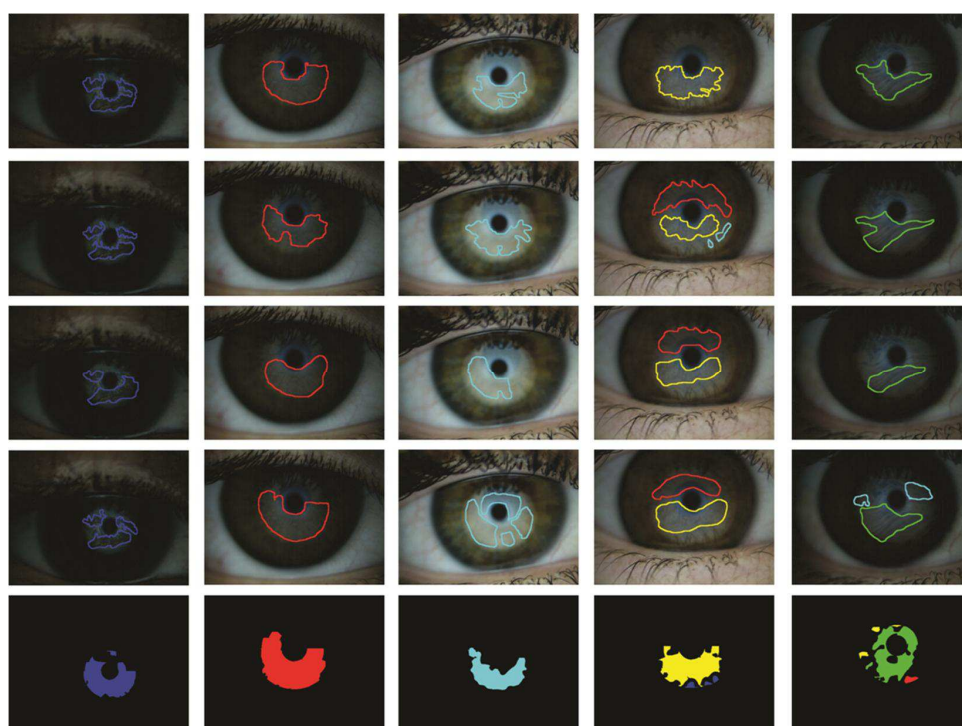


Figure 5. Annotations made by the 4 observers over 5 representative images, and their respective output images provided by the automatic system.

### 3. RESULTS

Table 1 shows the descriptive statistics of the size of the EC area (amount of pixels) for each observer irrespective of the LLP.

Table 1. Descriptive statistics of size areas quantified in pixels of area for each observer irrespective of lipid layer pattern. Median and interquartile range (IQ) are indicated. “*Erroneous categorization*” means those pixels that reference observer agreed with 0 observers or were marked only by the reference observer. \*Observer 5 refers to the automatic system.

Amount of pixels EC. Median (IQ)				
Observer 1	Observer 2	Observer 3	Observer 4	Observer 5*
2416 (3773)	1829 (3617)	6354 (8282)	1509 (2841)	3360 (5015)

In order to assess whether there were statistical differences between observers’ categorization, a Friedman test was used, and there was found a difference between them ( $p < 0.001$ ). Wilcoxon test was used to check pair differences between observers (table 2) and it was found that observer 3 showed a size of EC area significantly higher than the remaining 4 observers ( $p \leq 0.006$  for all comparisons, table 2), indicating that observer 3 categorized worse than the remaining observers. There was also a statistical difference between observer 4 and new application categorization ( $p < 0.044$ )

Table 2. Wilcoxon test outcomes. Pair wise comparisons between the amount of EC pixels categorized by two observers. In each comparison median of differences and level of statistical significance ( $p$ ) are indicated. *EC*: “*Erroneous categorization*”, means those pixels that reference observer agreed with 0 observers or were marked only by the reference observer. \*Observer 5 refers to the automatic system

Pair wise comparisons. Lipid layer pattern categorization					
	Observer 1	Observer 2	Observer 3	Observer 4	Observer 5*
Observer 1					
Observer 2	P = 0.26				
Observer 3	P = 0.01	P = 0.006			
Observer 4	P = 0.09	P = 0.50	P < 0.001		
Observer 5*	P = 0.55	P = 0.51	P = 0.003	P = 0.04	

Finally, it was compared the LLP categorization between observers for each LLP. This was done in order to find out whether the differences between the observers categorization were dependent on the LLP type. Table 3 shows the descriptive statistics of the size of the EC area (amount of pixels) categorized by each observer for each LLP. Friedman test showed that there were statistically significant differences between observers only for open meshwork LLP ( $p = 0.02$ ), but that was not true for the remaining LLPs; closed meshwork ( $p = 0.19$ ), wave ( $p = 0.39$ ), amorphous ( $p = 0.41$ ) and color fringe ( $p = 0.19$ ). In this case pair wise comparisons (Wilcoxon test) was only done for OM pattern, because this was the only LLP that showed differences between observers. Table 4 shows the Wilcoxon test for open meshwork LLP and it was found that there were significant differences only when comparing the size of EC area between observer 1 and observer 4 ( $p = 0.01$ ) and between observer 4 and the automatic system ( $p = 0.02$ ).

Table 3. Descriptive statistics of the size of the EC area (amount of pixels) categorized by each observer for each LLP. Median and interquartile range (IQ) are indicated. *EC*: “*Erroneous categorization*”, means those pixels that reference observer agreed with 0 observers or were marked only by the reference observer. \*Observer 5 refers to the automatic system.

	Amount of pixels EC. Median (IQ)				
	Observer 1	Observer 2	Observer 3	Observer 4	Observer 5*
Open meshwork	4234 (9489)	1820 (5602)	10144 (8660)	1328 (2236)	5503 (4284)
Closed meshwork	3350 (5778)	2795 (3650)	4780 (16017)	1417 (2446)	4130 (4402)
Wave	2819 (1690)	1720 (3271)	5684 (15277)	3369 (9278)	2592 (7920)
Amorphous	717 (2102)	770 (3432)	3308 (7747)	1314 (3921)	2174 (3387)
Color fringe	3155 (4145)	1586 (8338)	7267 (21206)	1223 (1558)	3134 (7795)

Table 4. Wilcoxon test outcomes for Open meshwork lipid layer pattern categorization. Pair wise comparisons between the amount of EC pixels categorized by two observers. In each comparison median of differences and level of statistical significance ( $p$ ) are indicated. *EC*: “*Erroneous categorization*”, means those pixels that reference observer agreed with 0 observers or were marked only by the reference observer. \*Observer 5 refers to the automatic system.

**Pair wise comparisons. Lipid layer pattern categorization**

	Observer 1	Observer 2	Observer 3	Observer 4	Observer 5*
Observer 1					
Observer 2	P = 0.21				
Observer 3	P = 0.09	P = 0.21			
Observer 4	P = 0.09	P = 0.12	<b>P = 0.01</b>		
Observer 5*	P = 0.67	P = 0.48	P = 0.12	<b>P = 0.02</b>	

#### 4. CONCLUSION

This study showed a new automatic tool, within the framework iDEAS, to identify several LLP zones in a single patient image. In a previous research,[8] a preliminary study showed that the automatic system showed similar categorization than observers, especially for CO and OM LLPs, whereas W pattern showed less percentage of coincidences.[8] In the present study the automatic application was validated by comparing its performance against new four experienced observers.

Categorizations of LLP zones were compared between the 5 observers. In general, observer 3 classified worse than the remaining 4 observers (tables 1 and 2) and the automatic system was classified worse only when comparing with the observer 4 (observer 4 was the most conservative). However, these differences were found only for the OM pattern (tables 3 and 4), so in the remaining lipid layer categories there was a consistency between observers in the examination of the LLP areas.

From the results found here, the automatic application is able to provide zones similar to the annotations made by experienced optometrists. Thus, the manual process done by experts can be automated with the benefits of being unaffected by subjective factors. This new software clearly improves the previous automatic application that was designed to categorize the whole pattern.[5] However, there is still large room for improvement on the processing time needed to generate the output image (10 minutes on average). Consequently, our future research will involve developing an optimized version whose processing time makes it useful in any clinical routine.

As an interferential phenomena, the LLPs are related to colors appearance, and some authors only addressed the color of the pattern.[3, 15] The authors considered that the best way to address the LLPs is by doing an analysis based in both texture and color. However, the lipidic reflection does not always show a CO pattern. The observation of a colorless pattern (grey color) is because its thickness is below the minimal thickness to produce interference fringes. Korb established the lipid layer thickness that corresponded to each color[3] as well as Isenberg et al.[16] From those classifications it can be seen that thinner LLPs (from OM to W) showed a grey background, and yellow color begins to appreciate in the transition of W and A patterns. In our experience,[5] we have noted that the thicker the lipid layer, the more marked appear the details of the pattern. Thus, as the lipid layer gets thicker, the pattern produced goes through the following stages: almost no details on a dark background (OM); changing to clearly visible dark streaks on an ever-brighter grey background followed by the merging of streaks to form large zig-zags (CM); until they thin out, and give

rise to the flow wave pattern (W); the gray background then turns yellowish until waves disappear to give the amorphous pattern (AM); and finally on this yellow background, appear the first brown/blue colors (CO).

In conclusion, the automatic application included in the framework iDEAS is able to categorize LLP zones as done by experienced optometrists. This device offers a clear benefit in categorizing the heterogeneity of the LLP without being affected by subjective factors.

## ACKNOWLEDGMENTS

This study was funded by the Spanish Ministry of Science and Education and the Institute of Health Carlos III (ISCIII) through research project PI10/01098.

## REFERENCES

- [1] J. P. Guillon, "Non-invasive Tearscope Plus routine for contact lens fitting," *Cont Lens Anterior Eye*, 21 Suppl 1, S31-40 (1998).
- [2] J. P. Guillon, "Abnormal lipid layers. Observation, differential diagnosis, and classification," *Adv Exp Med Biol*, 438, 309-13 (1998).
- [3] D. R. Korb, [The tear film-its role today and in the future.], (2002).
- [4] J. J. Nichols, K. K. Nichols, B. Puent *et al.*, "Evaluation of tear film interference patterns and measures of tear break-up time," *Optom Vis Sci*, 79(6), 363-9 (2002).
- [5] C. Garcia-Resua, M. J. Giraldez Fernandez, M. F. Gonzalez Penedo *et al.*, "New software application for clarifying tear film lipid layer patterns," *Cornea*, 32(4), 538-46 (2013).
- [6] "The definition and classification of dry eye disease: report of the Definition and Classification Subcommittee of the International Dry Eye WorkShop (2007)," *Ocul Surf*, 5(2), 75-92 (2007).
- [7] S. Aydogdu, K. Ertekin, A. Suslu *et al.*, "Optical CO<sub>2</sub> sensing with ionic liquid doped electrospun nanofibers," *J Fluoresc*, 21(2), 607-13 (2011).
- [8] B. Remeseiro, N. Barreira, C. Garcia-Resua *et al.*, "iDEAS: A web-based system for dry eye assessment," *Comput Methods Programs Biomed*, 130, 186-97 (2016).
- [9] B. Remeseiro, M. Penas, A. Mosquera *et al.*, "Statistical comparison of classifiers applied to the interferential tear film lipid layer automatic classification," *Comput Math Methods Med*, 2012, 207315 (2012).
- [10] B. Remeseiro, M. Penas, N. Barreira *et al.*, "Automatic classification of the interferential tear film lipid layer using colour texture analysis," *Comput Methods Programs Biomed*, 111(1), 93-103 (2013).
- [11] B. Remeseiro, L. Ramos, N. Barreira *et al.*, "Colour texture segmentation of tear film lipid layer images." 8112, 140-141.
- [12] B. Remeseiro, M. Penas, N. Barreira *et al.*, "Automatic classification of the interferential tear film lipid layer using colour texture analysis," *Comput Methods Programs Biomed*, 111(1), 93-103 (2013).
- [13] K. McLaren, "The development of the CIE 1976 (L\*a\*b) uniform colour-space and colour-difference formula," *J Soc Dyers Colourists*, 92(9), (1976).
- [14] R. M. Haralick, K. Shanmugam, and I. Dinstein, [Textural features for image classification], (1973).
- [15] E. Goto, M. Dogru, T. Kojima *et al.*, "Computer-synthesis of an interference color chart of human tear lipid layer, by a colorimetric approach," *Invest Ophthalmol Vis Sci*, 44(11), 4693-7 (2003).
- [16] S. J. Isenberg, M. Del Signore, A. Chen *et al.*, "The lipid layer and stability of the precocular tear film in newborns and infants," *Ophthalmology*, 110(7), 1408-11 (2003).